



This is a repository copy of *Characteristics of Multi-Component Formulation Granules Formed using Distributive Mixing Elements in Twin Screw Granulation*.

White Rose Research Online URL for this paper:
<http://eprints.whiterose.ac.uk/134434/>

Version: Accepted Version

Article:

Pradhan, S.U., Sen, M., Li, J. et al. (4 more authors) (2018) Characteristics of Multi-Component Formulation Granules Formed using Distributive Mixing Elements in Twin Screw Granulation. *Drug Development and Industrial Pharmacy*, 44 (11). pp. 1826-1837. ISSN 0363-9045

<https://doi.org/10.1080/03639045.2018.1503293>

Reuse

Items deposited in White Rose Research Online are protected by copyright, with all rights reserved unless indicated otherwise. They may be downloaded and/or printed for private study, or other acts as permitted by national copyright laws. The publisher or other rights holders may allow further reproduction and re-use of the full text version. This is indicated by the licence information on the White Rose Research Online record for the item.

Takedown

If you consider content in White Rose Research Online to be in breach of UK law, please notify us by emailing eprints@whiterose.ac.uk including the URL of the record and the reason for the withdrawal request.



eprints@whiterose.ac.uk
<https://eprints.whiterose.ac.uk/>

Characteristics of Multi-Component Formulation Granules Formed using Distributive Mixing Elements in Twin Screw Granulation

Shankali U. Pradhan ^a, Maitraye Sen ^a, Jiayu Li ^a, Ian Gabbott ^c, Gavin Reynolds ^c, James D. Litster ^d, Carl R. Wassgren ^{b, c *}

a Davidson School of Chemical Engineering, Purdue University, 480 Stadium Mall Dr., West Lafayette, IN 47907, USA

b School of Mechanical Engineering, Purdue University, 585 Purdue Mall, West Lafayette, IN 47907, USA

c Department of Industrial and Physical Pharmacy, Purdue University, 575 Stadium Mall Dr., West Lafayette, IN 47907, USA

d Department of Chemical and Biological Engineering, University of Sheffield, Mappin Street, Sheffield S1 3JD, UK

e Pharmaceutical Technology and Development, AstraZeneca, Silk Road Business Park Charter Way, Macclesfield, Cheshire SK10 2NA, UK

* Corresponding author

Contact information of authors:

Shankali U. Pradhan: shankali.pradhan@gmail.com, Maitraye Sen: maitraye.sen@gmail.com,

Jiayu Li: li1722@purdue.edu, Ian Gabbott: Ian.Gabbott@astrazeneca.com, Gavin Reynolds:

Gavin.Reynolds@astrazeneca.com, James D. Litster: james.litster@sheffield.ac.uk, Carl R.

Wassgren: wassgren@purdue.edu

ABSTRACT

This work examines the influence of pharmaceutical formulation characteristics on granule properties formed using distributive mixing elements (DMEs) in twin screw granulation. High and low drug dose formulations with three different active pharmaceutical ingredients (APIs) were considered. The type and concentration of the API in the formulation significantly affected the dry blend particle size distribution and the wet blend dynamic yield strength. However, despite the differences in blend properties, the granule size distributions were not significantly affected by the type of API used. The granule size distributions were solely functions of the liquid-to-solid ratio and the screw element geometry. However, the granule porosities were observed to be dependent on both the liquid-to-solid ratio and the dynamic yield strength of the blends.

Keywords: Distributive mixing elements, twin screw granulation, dynamic yield strength, granule breakage.

1. Introduction

The Twin Screw Granulator (TSG) is becoming increasingly considered for the continuous manufacture of pharmaceutical products due to its compact size, flexible design, wide range of capacities, and short residence time [1,2]. A TSG offers processing condition flexibility such as screw speed, powder feed rate, liquid-to-solid ratio (L/S ratio), and screw configuration for a wide variety of formulations. The effects of L/S ratio, powder feed rate, screw configurations, and screw speed have been previously reported in the literature [3–10]. However, little is known about the effects of formulation changes on granule properties using various screw designs.

Literature reports focused on understanding granulation using different screw designs have shown that granule properties are sensitive to the screw element geometry. Conveying elements are known to be low shear transport elements that result in bimodal granule size distributions characterized by large, porous granules and a significant mass of fines [8,11]. The maximum granule size from conveying elements is a strong function of the pitch of the screw [8]. Distributive mixing elements (DMEs) cut and combine the wet mass, resulting in better liquid distribution compared to conveying elements and monomodal granule size distributions [12]. DMEs produce rounded granules with high porosity. The adjacent reverse DME configuration has been found to give the best granule properties compared to other DME configurations [13]. Kneading elements have been classified as high shear elements that produce dense, elongated granules with good liquid distribution of the wet mass [12,14,15]. They cause mixing of the wet mass by shear elongation and breakage, followed by layering with adjacent dry powder particles. The reverse kneading element configurations show improved liquid distribution compared to the forward configurations [14]. We have chosen distributive mixing elements for the purposes of this study as these screw elements result in the best granule properties for downstream pharmaceutical tableting in terms of the desired size distribution, shape, and porosity.

Any wet granulation operation involves three rate processes [16]:

- 1) Nucleation and wetting
- 2) Coalescence and consolidation

3) Breakage and attrition

Previous reports on twin screw granulation have shown that nucleation of powder with the binder and breakage of the wet powder mass are the dominant rate processes in a TSG [13,17]. Studies for high shear wet granulation show that formulation properties have an effect on nucleation as well as breakage. Nucleation of the powder bed with the binder is a strong function of the powder Sauter mean diameter, powder bed porosity, binder viscosity, surface tension, and contact angle [18]. The effects of formulation properties on nucleation have been characterized using the drop penetration time in a powder bed, modeled using the relation [16]:

$$t_p = 1.35 \frac{V_d^{2/3}}{\varepsilon_{eff}^2 R_{eff}} \frac{\mu}{\gamma_{LV} \cos \theta} \quad Eq (1)$$

where, t_p is the drop penetration time, μ is the liquid dynamic viscosity, ε_{eff} is the effective bed porosity, R_{eff} is the effective bed pore radius, γ_{LV} is the liquid surface tension, θ is the solid-liquid contact angle, and V_d is the volume of the penetrating drop. The parameters R_{eff} and ε_{eff} are given by [16]:

$$R_{eff} = \frac{\varphi d_{3,2}}{3} \frac{\varepsilon_{eff}}{1 - \varepsilon_{eff}} \quad Eq (2)$$

$$\varepsilon_{eff} = \varepsilon_{tap} (1 - \varepsilon + \varepsilon_{tap}) \quad Eq (3)$$

where, φ is the particle sphericity, $d_{3,2}$ is the Sauter mean diameter, ε is the loose packed powder bed voidage, and ε_{tap} is the tapped powder bed voidage.

Similarly, the breakage rate is a function of the powder particle size, binder viscosity, binder surface tension, granule saturation, and granule porosity [19–22]. The effects of formulation properties on breakage have been characterized using the dynamic yield strength (DYS) [19]. The DHS of the granules increases with increasing binder viscosity and decreasing Sauter mean diameter and granule porosity [19].

The dependence of granule characteristics on the formulation properties has been studied to a certain degree in the twin screw granulation literature. The primary particle sizes in the formulation have been shown to have a subtle effect on granule size distribution in kneading elements [17,23]. It is hypothesized that formulations with larger particle sizes result in denser granules due to increased deformability of the material [17]. In a multicomponent formulation,

changing the wettability or the relative concentration of a certain component tends to alter the powder-binder wettability of the entire formulation [24,25]. These differences are reflected in the final granule size distribution if the wetting properties are altered significantly [24]. Changing formulation wettability has no significant effect on the final granule size and homogeneity when foam granulation using kneading elements is used [25–27]. Certain commonly used excipients, such as microcrystalline cellulose, have a tendency to absorb some water within its structure. The water absorption capacity, which is closely linked to the crystallinity of the cellulose, decreases the effective mass of liquid available for granulation (if not compensated for) and results in a larger fraction of fines in the granule size distribution [28,29]. Increasing the binder concentration in the liquid phase decreases the mass of fines in the final granule size distribution and results in more homogeneous binder distribution using kneading elements [17]. However, in conveying elements, increasing binder viscosity results in a more heterogeneous liquid distribution, reflected as larger mass fractions of large lumps and fines [4]. Mostly, the reported studies in the twin screw granulation literature have not directly measured the impact of formulation changes on granule properties related to the granulation rate processes such as drop penetration time and dynamic yield stress.

As mentioned previously, distributive mixing elements give broad, monomodal granule size distributions and rounded, high porosity granules. Distributive mixing elements can produce granules with good liquid distribution without adversely affecting granule shape and porosity, unlike kneading elements [13]. There has been little study of the impact of formulation properties on the final granule attributes of different industrially relevant multicomponent formulations using distributive mixing elements. In this work, the effects of API particle size and concentration on the final granule characteristics using distributive mixing elements have been studied.

2. Materials and Methods

2.1. Materials

Three different active pharmaceutical ingredients (APIs) were considered for blend preparation: caffeine (BASF, Germany), micronized acetaminophen (micronized APAP) (Mallinckrodt, Derbyshire, UK), and semifine acetaminophen (semifine APAP) (Mallinckrodt, Derbyshire, UK). The high drug-load formulations consisted of 70.0% API, 16.5% mannitol (Pearlitol 160C,

Roquette Pharma, Lestrem, France), 5.4% microcrystalline cellulose (Avicel PH101, FMC Biopolymer, Wallingstown, Ireland), 5.1% sodium starch glycolate (Glycolys, Roquette Pharma, Lestrem, France), and 3.0% hydroxypropyl cellulose (Klucel EXF Pharm, Ashland, Hopewell, USA). The low drug-load formulations consisted of 30.3% API, 46.5% mannitol, 12.5% microcrystalline cellulose, 5.1% sodium starch glycolate, and 3.0% hydroxypropyl cellulose. The granulating liquid used for all the experiments was deionized water with 0.1% w/w Nigrosin dye. All dry powders were mixed in a Tote blender (Tote Systems, Fort Worth, USA, 5 L volume, fill level $\sim 2/3^{\text{rd}}$ of total blender volume) at 16 RPM for 40 minutes with a sieving step after the first 20 minutes using a 4 mm sieve to break up any large lumps. Twenty metal beads (12.7 mm diameter) were added to the mixture during blending to prevent the formation of large agglomerates.

2.2.API particle size distribution and particle shape

The particle size distributions for each API and excipient were measured using a wet dispersion laser diffraction technique (Malvern Mastersizer 2000 Light Diffraction Particle Size Analyzer). A saturated solution of acetaminophen in deionized water was used as the dispersant for both micronized and semifine APAP and a saturated solution in ethanol was used as the dispersant for caffeine, mannitol, and microcrystalline cellulose. The particle size distributions of sodium starch glycolate and hydroxypropyl cellulose were not measured as these materials tend to swell during wet granulation. Three replicate measurements were performed on samples obtained from different locations in the bulk. The shape of the API particles was measured by microscopy imaging of particles dispersed on a glass slide using a Malvern Morphologi G3SE-ID. Air at 5 bar pressure was used to disperse the API on a glass plate prior to imaging, to ensure deagglomeration of the API. API solubility in the granulating liquid was determined using data from the literature [30,31].

2.3.Blend flow property measurements

The bulk and tapped densities of the blends were measured using a graduated measuring cylinder and three replicate measurements were performed for each blend. For tapped density measurements, the powder bed was subjected to 2000 taps using an Agilent 350 Tapped Density analyzer. The Hausner ratio was calculated using the bulk and tapped densities.

2.4.Drop penetration time

The powder bed for drop penetration time measurements was prepared using the FT4 Powder Rheometer (Freeman Technology, Gloucestershire, UK). The powder sample was placed in a 50 mm x 80 ml split vessel and was subject to seven conditioning cycles using the 50 mm blade, followed by splitting of the powder bed to obtain a smooth powder surface. A 20 ml syringe with a 1.6 mm ID syringe tip was filled with deionized water as the granulating liquid and held in place at a distance of 20 mm above the powder surface using a clamp. Single drops were released from the syringe on the powder surface. A high speed camera (Photron Fastcam- X 1024 PCI) was used to record drop penetration into the powder bed. The drop penetration time was determined using ImageJ 1.51h software. Five replicate measurements were performed for each sample.

2.5.Dynamic yield strength (DYS)

For the DYS measurement, the powder (blend) and the granulating liquid (water) were mixed in a plastic bag at the desired L/S ratio and cylindrical pellets of diameter 25 mm (diameter = height) were prepared using a hand punch and die set to give the desired solid fraction. The DYSs for the blends were measured at liquid-to-solid (L/S, w/w) ratios of 0.25, 0.35, and 0.45 and a bed solid fraction of 0.58. Pellets that would hold together under gravity at L/S ratios smaller than 0.25 could not be formed due to insufficient granulating liquid. L/S ratios larger than 0.45 resulted in near slurries. Hence, the only the range from 0.25 to 0.45 was considered for DYS measurements.

The solid fraction of 0.58 was chosen since it is approximately the same as the average solid fraction of the granules produced. The L/S ratio and solid fraction of the pellets were maintained within 10% of the target value. The DYS was measured using an Instron ElectroPuls E1000 material testing system with a platen impact speed of 10 mm/s. Actual particle impact speeds in the TSG under the operating conditions in this work are not known. Typical particle impact speeds in a high shear batch granulator have been estimated to be 10-20% of the impeller tip speed [22,32,33]. Hence, the platen speed used in this study is of the same order of magnitude as 10% of the screw tip speed. The detailed methodology for measuring the DYS is given elsewhere [34]. The results are plotted as the average of at least three replicate experiments with \pm 95% confidence interval as a scatter bar.

2.6. Twin Screw Granulation experiments

The granulation experiments were performed in a EuroLab 16 mm 25:1 length:diameter ratio TSG (Thermo Fisher Scientific, Karlsruhe, Germany). The TSG is divided into six sections, each with a length of 60 mm and an end section, which has a length 20 mm. A schematic of the experimental set-up is shown in Figure 1.

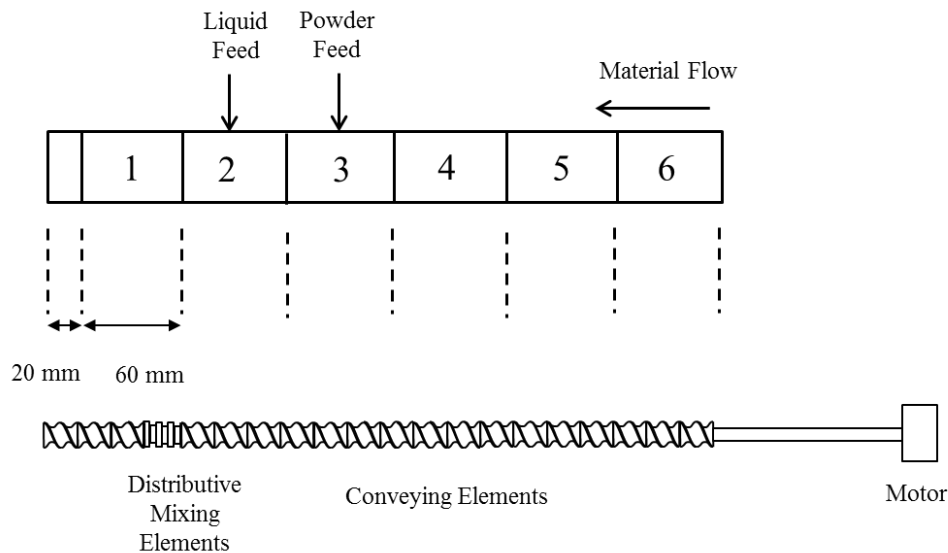


Figure 1: Experimental set up for the twin screw granulation experiments using Distributive Mixing Elements. Sections 1 to 6 have a length of 60 mm each.

The screw configuration consisted of three pairs of distributive mixing elements (DMEs) placed in an adjacent-reverse configuration [13] with three pairs of double-flighted 1 L/D (length/diameter) conveying elements placed downstream to promote granule layering. The powder was fed using a gravimetric feeder (Brabender Technologie, ON, Canada) and the granulating liquid was fed using a Masterflex peristaltic pump at appropriate flow rates to achieve the desired L/S ratio. All experiments were performed at a 4 kg/h powder flow rate. The experiments for 30% API blends were performed at a screw speed of 400 RPM whereas a screw speed of 800 RPM was used for all of the 70% API blends granulation experiments. The 70% API blends were cohesive and difficult to flow (Section 3.1) and, thus, a screw speed of 800 RPM was required to prevent bridge formation and powder backup in the powder feed port. Although the screw speeds for the granulation of 30% and 70% API blends were different, it is known in case of conveying and kneading elements that screw speed does not have a significant

effect on the final granule size distribution [9]. The granules were tray dried for 48 h prior to further characterization.

2.7. Granule/blend size distribution

The granule and dry blend size distribution was measured by sieve analysis using sieves ranging from 63 μm to 8 mm in a $\sqrt{2}$ geometric series. The size distributions were plotted as the normalized mass frequency distribution of the logarithm of the particle size:

$$f_i(\ln x) = \frac{y_i}{\ln(\bar{x}_{i+1}/\bar{x}_i)}, \quad \text{Eq. (4)}$$

where y_i is the mass fraction in size interval i and \bar{x}_i is the mean sieve size corresponding to interval i .

2.8. Granule porosity

The skeletal density of the granules was measured using an Accupyc II 1340 helium pycnometer (Micromeritics, GA, USA) followed by envelope density measurements performed using the Geopyc 1360 powder pycnometer (Micromeritics, GA, USA). The granules in the size fraction 1.0 – 1.4 mm were chosen for porosity measurements as it is the smallest granule size for accurate measurement using the powder pycnometer. The granules were placed in a desiccator for at least 8 h prior to the measurement to minimize the interference of moisture during the analysis. The porosity of granules was calculated using the skeletal and envelope densities:

$$\varepsilon_{granules} = 1 - \frac{\rho_e}{\rho_s} \quad \text{Eq. (5)}$$

where ρ_e and ρ_s are the envelope and skeletal densities, respectively. The average result of three replicate experiments has been reported.

3. Results and Discussion

3.1. Raw Material Characterization

The raw material particle size analysis is described elsewhere [35], but is repeated here for the reader's convenience. The particle size analyses of the three APIs and the excipients with $\pm 95\%$ confidence interval are given in Table 1. The corresponding volume frequency distributions are shown in Figure 2.

Size distribution parameter (μm)	Micronized APAP	Semifine APAP	Caffeine	Mannitol	MCC
$d_{3,2}$ (Sauter mean diameter)	7.2 ± 0.7	23.2 ± 4.9	9.2 ± 3.1	54.3 ± 7.6	83.4 ± 0.4
$d_{4,3}$ (weighted average volume diameter)	23.6 ± 2.8	98.8 ± 16.0	40.3 ± 5.9	191.2 ± 22.3	28.8 ± 1.6
d10	5.4 ± 0.9	18.3 ± 2.5	11.0 ± 7.6	38.9 ± 2.7	21.9 ± 0.2
d50 (median)	20.5 ± 2.7	71.9 ± 12.5	36.1 ± 4.0	140.8 ± 9.8	72.9 ± 1.3
d90	46.0 ± 5.0	210.9 ± 39.3	75.0 ± 7.7	422.3 ± 59.4	160.5 ± 2.9

Table 1: Particle size distribution parameters, measured using laser diffraction, for the APIs and excipients. All measurements are in units of microns. The average of three replicates with $\pm 95\%$ confidence interval is given.

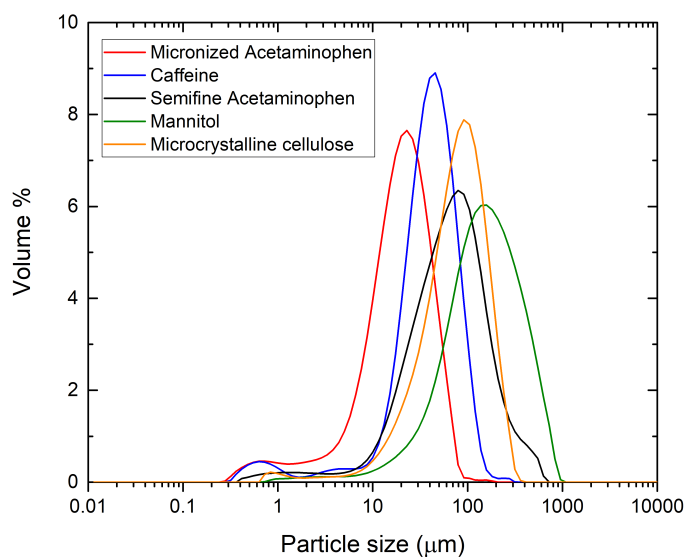


Figure 2: Volume based particle size distributions, measured using laser diffraction, for the APIs and excipients.

The particle size distribution analyses of the APIs show that semifine APAP has the largest average particle size whereas micronized APAP has the smallest average particle size among the three APIs (see Table 1 and figure 2). Furthermore, the semifine APAP size distribution is

broader ($\text{span} = \frac{d_{90}-d_{10}}{d_{50}} = 2.68$) compared to the micronized APAP ($\text{span} = 1.98$) and the caffeine distribution ($\text{span} = 1.77$). The Sauter mean diameter is an important measure of particle size distribution because it is reflected in the drop penetration time model and the DYS as described in Section 1. The Sauter mean diameter of the semifine APAP is larger than the micronized APAP and caffeine. The average particle size of the mannitol is larger than all three APIs, while the MCC has a size distribution similar to the semifine APAP. It is worth noting that the Sauter mean diameter of MCC is larger than the semifine APAP.

Table 2 lists the solubility and the particle shape parameters for the three APIs considered. The variations in circularity and aspect ratio indicate minor differences in the particle shape and these differences are not expected to affect the blend properties considerably. Caffeine has a larger solubility in water, which is the granulating liquid used for the wet granulation experiments. Thus, caffeine is expected to have a stronger tendency for solubilization during wet granulation of the caffeine blends and consequent recrystallization during the drying of the wet granules.

API	Circularity	Aspect ratio	Solubility in water (g/L at 25°C)
Caffeine	0.58 ± 0.11	0.61 ± 0.03	21
Micronized APAP	0.62 ± 0.03	0.61 ± 0.04	14
Semifine APAP	0.59 ± 0.12	0.57 ± 0.14	14

Table 2: Average particle shape parameters with ± 95% confidence interval from three replicate experiments, and solubility in water for caffeine, micronized APAP, and semifine APAP [30,31].

The bulk and tapped densities of the 30% and 70% API blends are listed in Table 3. Although the bulk and tapped densities of the 30% blends are somewhat larger than the 70% blends, the Hausner ratios of all the blends are similar. The Hausner ratio is a measure of flowability and as a rule of thumb, a Hausner ratio larger than 1.25 indicates poorly flowing powder. According to the Hausner ratio, all of the blends are poorly flowing materials. This result was particularly evident during feeding of the material into the TSG. For the 70% blends, the feeder's rubber

hopper had to be lined with paper to reduce wall friction and improve the flow of the blend into the TSG. Furthermore, the screw speed for the twin screw granulation experiments of the 70% blends was set to 800 RPM instead of 400 RPM to break the formation of powder bridges in the powder feed port of the TSG. The 30% and 70% blends have similar bed porosity values. This result indicates that a variation in the API primary particle size or small differences in particle shape factors, as shown in Table 2, do not affect the packing of the particles in the bulk of the powder bed.

Blend name	Poured bulk density (g/ml)	Tapped density (g/ml)	Hausner ratio	Poured bed porosity	Tapped bed porosity
30% micronized APAP	0.40 ± 0.02	0.66 ± 0.03	1.63 ± 0.07	0.72 ± 0.02	0.54 ± 0.02
30% caffeine	0.45 ± 0.04	0.73 ± 0.03	1.62 ± 0.08	0.70 ± 0.02	0.51 ± 0.02
30% semifine APAP	0.45 ± 0.02	0.68 ± 0.03	1.50 ± 0.11	0.69 ± 0.02	0.53 ± 0.02
70% micronized APAP	0.254 ± 0.024	0.41 ± 0.03	1.61 ± 0.23	0.81 ± 0.02	0.70 ± 0.02
70% caffeine	0.33 ± 0.03	0.53 ± 0.03	1.61 ± 0.14	0.78 ± 0.02	0.64 ± 0.02
70% semifine APAP	0.301 ± 0.049	0.54 ± 0.02	1.81 ± 0.25	0.78 ± 0.04	0.60 ± 0.02

Table 3: Bulk and tapped densities of the 30% and 70% API blends. The average of three replicates with ± 95% confidence interval is shown.

Figure 3 shows the size distributions of the 30% and 70% APAP and caffeine dry blends measured by sieve analysis. Although the primary particle sizes of all three APIs are different, it is important to note that significant fractions of all three APIs are smaller than the smallest sieve size (63 μm) used in the analysis. Hence, it is expected that a fines peak will be observed at the smallest mean sieve size for all three APIs.

The 30% caffeine blend shows a larger fraction of - 63μm material than the 30% semifine APAP blend. The 30% micronized APAP blend shows a significantly smaller mass of fines than the 30% semifine and caffeine blends despite micronized APAP having the smallest primary particle size among the three APIs. Micronized APAP forms dry agglomerates that do not break during sieving. This effect is more evident in the 70% blends where a significant proportion of large agglomerates are observed, as the concentrations of the free-flowing excipients are significantly

smaller than in the 30% blends. The sieve analysis of the 70% caffeine blend shows a fines peak corresponding to the caffeine primary particle size. However, the 70% semifine and micronized APAP blends show a peak at a sieve size significantly larger than the primary particle size of the API due to dry agglomeration.

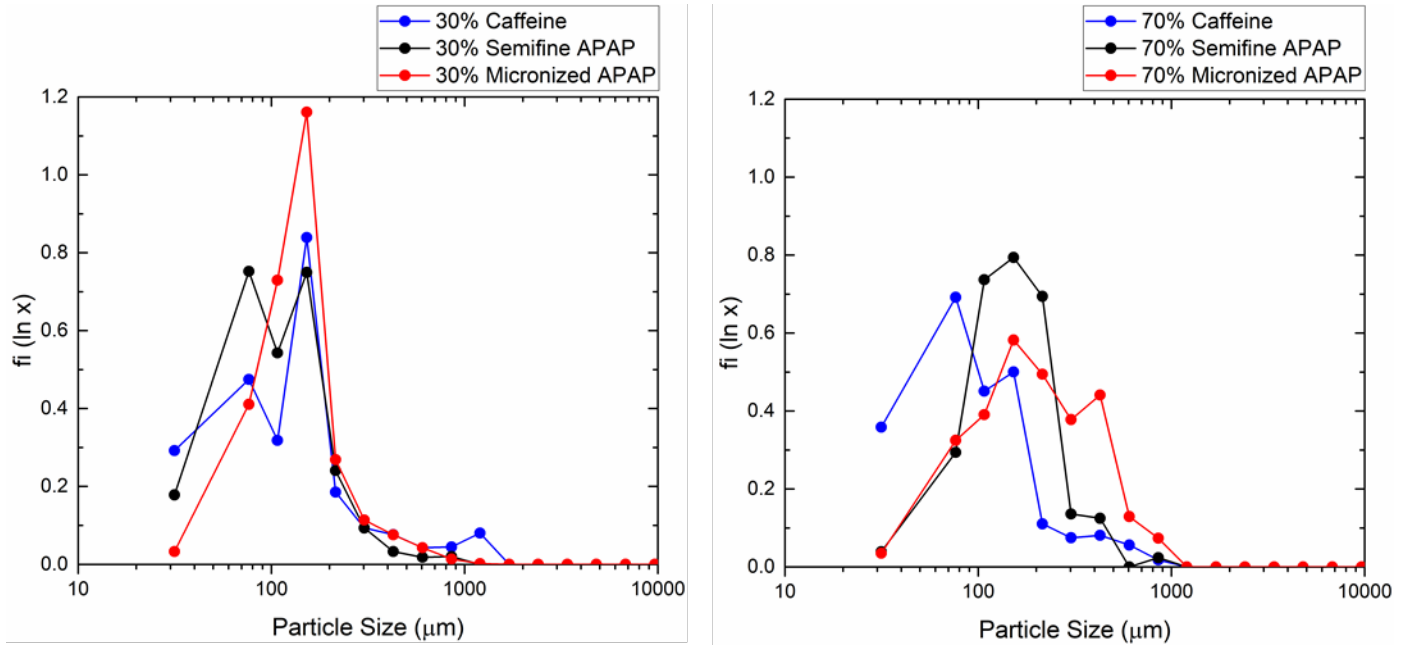


Figure 3: Sieve analyses of 30% and 70% API dry blends.

The experimentally measured drop penetration times and Sauter mean diameters of the six dry blends, calculated from the dry blend size distribution measured by sieve analysis (Figure 3), are given in Table 4.

Blend name	Drop penetration time (s)	Sauter mean diameter $d_{3,2}$ from dry blend sieve analyses (μm)
30% semifine APAP blend	5.0 ± 0.9	97.5
30% micronized APAP blend	5.7 ± 0.4	125.0
30% caffeine blend	5.0 ± 0.4	96.5
70% semifine APAP blend	5.3 ± 0.8	133.4

70% micronized APAP blend	5.3 ± 1.0	159.3
70% caffeine blend	5.4 ± 1.0	83.8

Table 4: Drop penetration times in the 30% and 70% API blends and Sauter mean diameters of dry blends obtained by sieve analysis. Drop penetration time data is shown as average of at least ten replicates ± one standard deviation

The drop penetration times for all the blends are similar. This result suggests that the nucleation rates in all the blends will be similar, and all blends are easily wet by the binder liquid. This result is surprising given the differences in API primary particle size distribution (Figure 2) and may be because of the presence of MCC or caffeine in the blends. The model described in Section 1 assumes that the liquid drop penetration is solely governed by the capillary suction in the powder bed, as given by the Washburn equation, and does not account for the liquid absorption by the powder particles [16]. It is known that MCC particles absorb water, rendering less water available for granulation [29]. It is also known that caffeine forms hydrate chains on contact with water [36]. It is likely that these factors influence the drop penetration time and may cancel the effects of the API particle size differences. Since the nucleation behavior of all the formulations considered in this work is expected to be similar, any differences in granule properties would be primarily due to differences in the breakage behavior.

Figure 4 shows the DYS values of the 30% and 70% API blends as functions of the L/S ratio. The DYS of the 30% caffeine blend is approximately two times larger than the 30% APAP blends, whereas the DYS of the 70% caffeine blend is approximately four times that of the 70% APAP blends. The micronized APAP blends have larger dynamic yield strengths than the semifine APAP blends for all of the L/S ratios considered. It is important to note that there are several factors that affect the particle-particle and particle-liquid interactions, which in turn, affect the DYS of the material. It is known that caffeine forms hydrate chains and it is possible that the nature and number of liquid bridges in the caffeine blends are significantly different than the APAP blends, resulting in differences in the DYS [36]. As stated in section 1, the granule breakage rate is a function of the DYS. The API blends in this work span a one order of

magnitude range of DYS values, and are ideal for studying the effect of granule strength on the breakage in TSG.

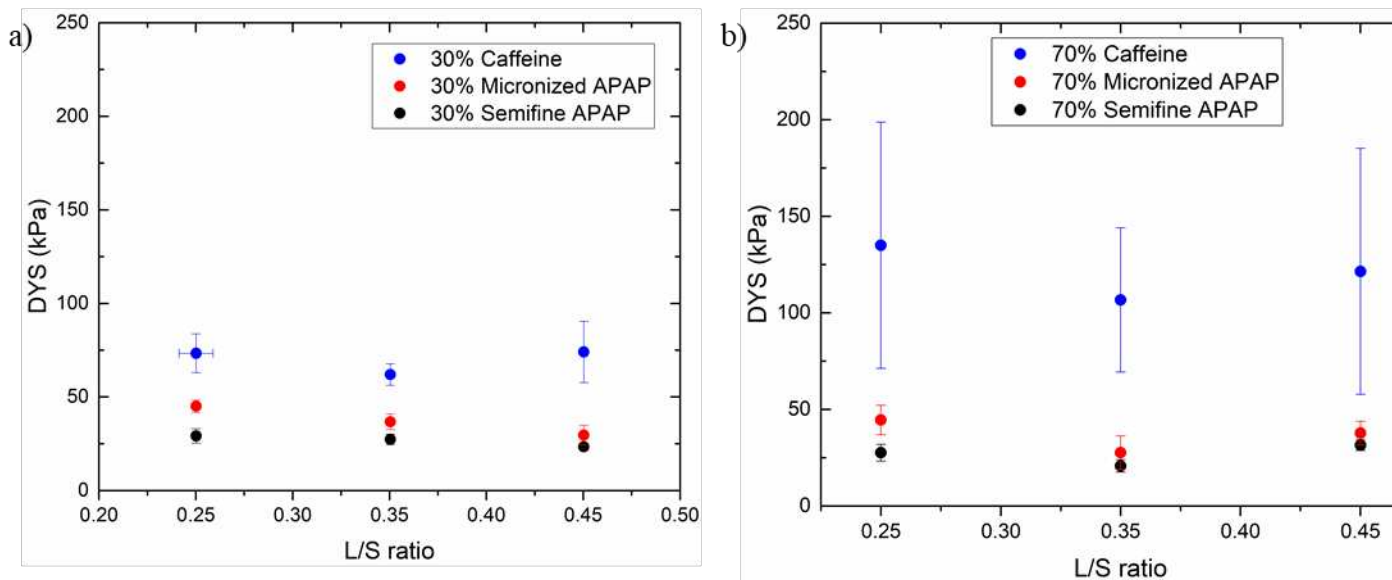


Figure 4: Dynamic yield strengths of a) 30% API blends and b) 70% API blends at different L/S ratios. Scatter bars represent \pm 95% confidence interval from at least three replicate measurements.

3.2. Effect of formulation properties on granule size distribution and porosity

The granule size distribution of the 30% and 70% API blends at four different L/S ratios are shown in Figure 5 and 8 respectively. Repeat experiments were performed for the 30% APAP blends to assess the reproducibility of the experiments and the data from the two replicate experiments were found to be similar. The average data are plotted in Figure 5 for plot clarity. The data from the two replicate experiments are shown in Figures 6 and 7. The size distribution shifts to the larger granule sizes as the L/S ratio increases. An increase in the L/S ratio results in increased availability of liquid for granulation, contributing to granule growth. The granule size distribution is monomodal and granules are obtained primarily in the size range of 100-2000 μm . This behavior is characteristic of distributive mixing elements [13].

Figures 5 and 8 show that both the choice of API, and the amount of API in the blend, have a much smaller impact on the granule size distribution than the L/S ratio, despite the DYS of the

granules made from these blends varying over one order of magnitude. In general, the granule mean size is higher for 30% blends than 70% blends, and caffeine blends gave higher mean size than the APAP blends (see Figure 9). These differences were statistically significant (see Tables 5 and 6). The 30% blends contain more MCC, which absorbs some of the moisture making it unavailable for granulation. We hypothesize that this is the main reason why granule mean size does not increase as rapidly with increasing L/S ratio for the 30% blends, compared to the 70% blends.

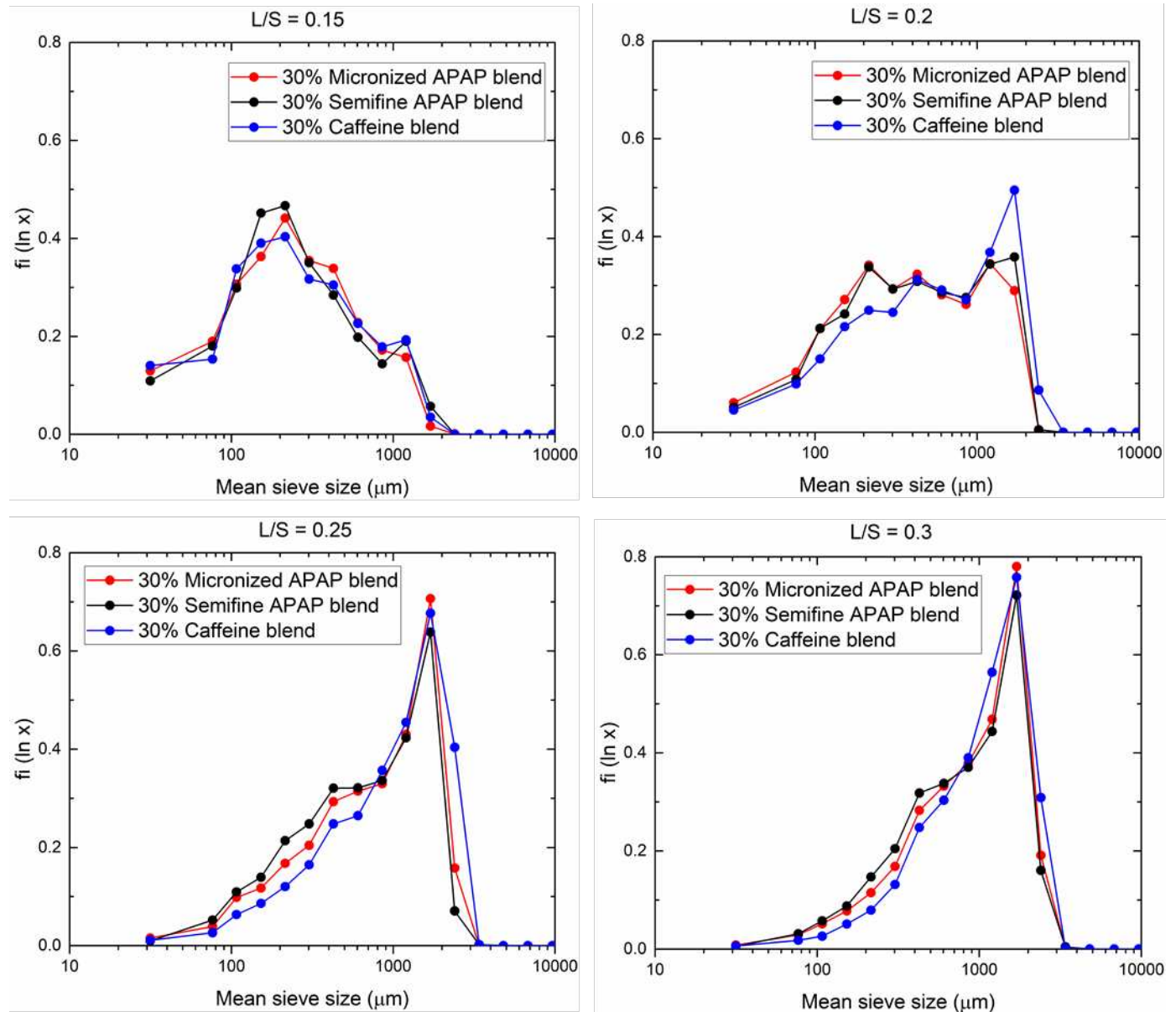


Figure 5: Granule size distributions of the 30% API blends at L/S ratios of 0.15, 0.2, 0.25, and 0.3 using distributive mixing elements. Average data is shown for plot clarity.

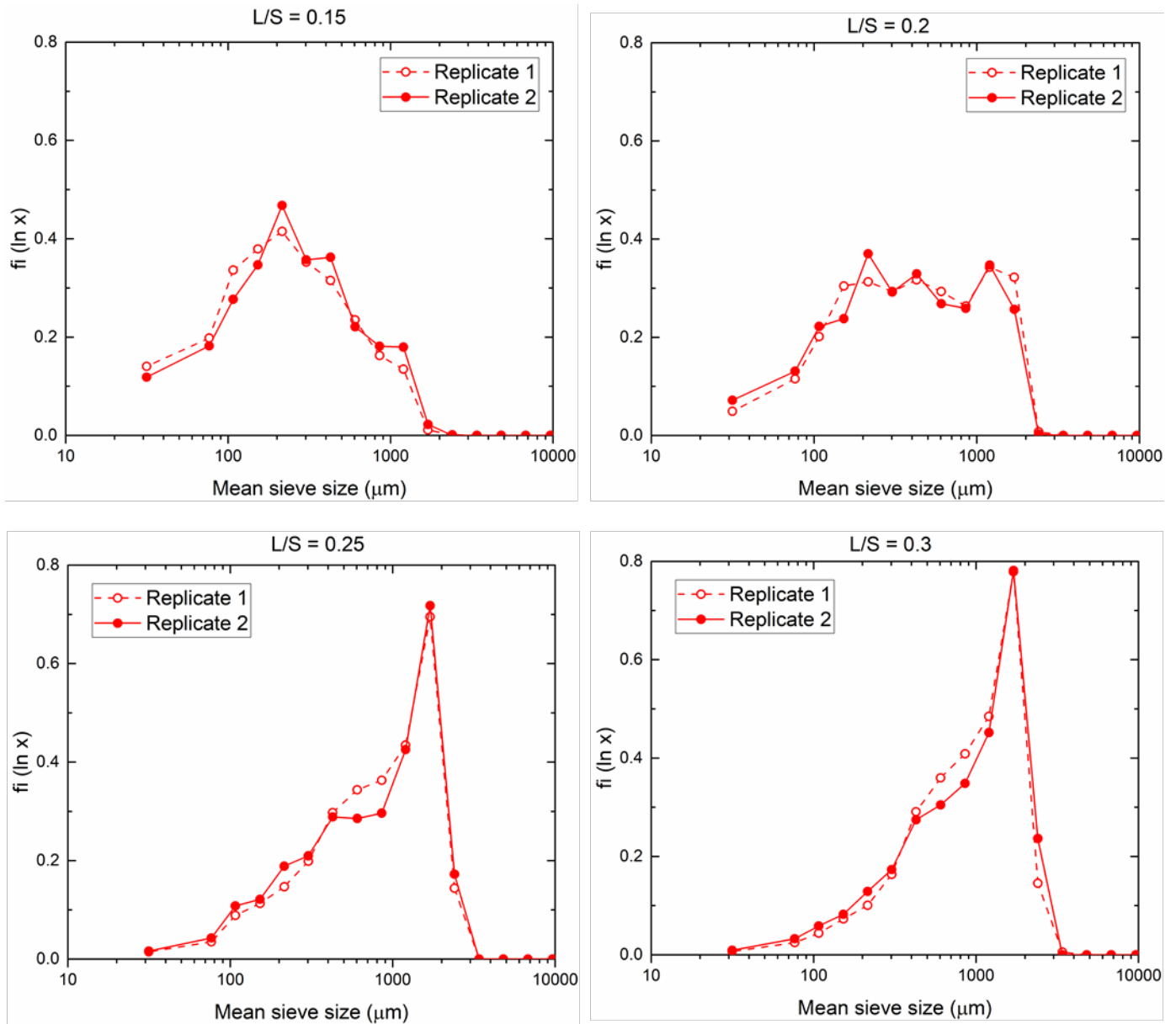


Figure 6: Comparison of replicate experiments for 30% micronized APAP blend at different L/S ratios

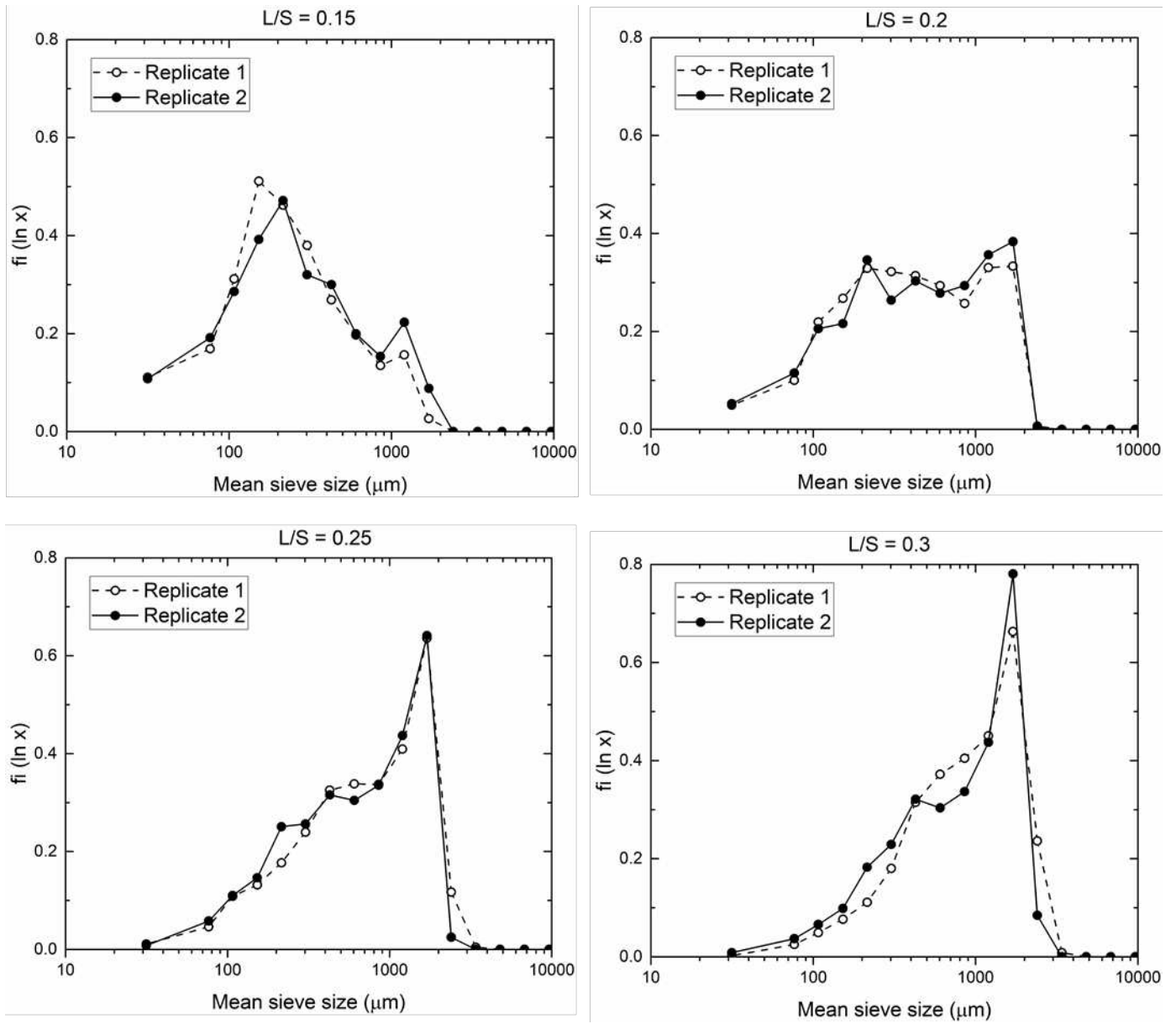


Figure 7: Comparison of replicate experiments for 30% semifine APAP blend at different L/S ratios

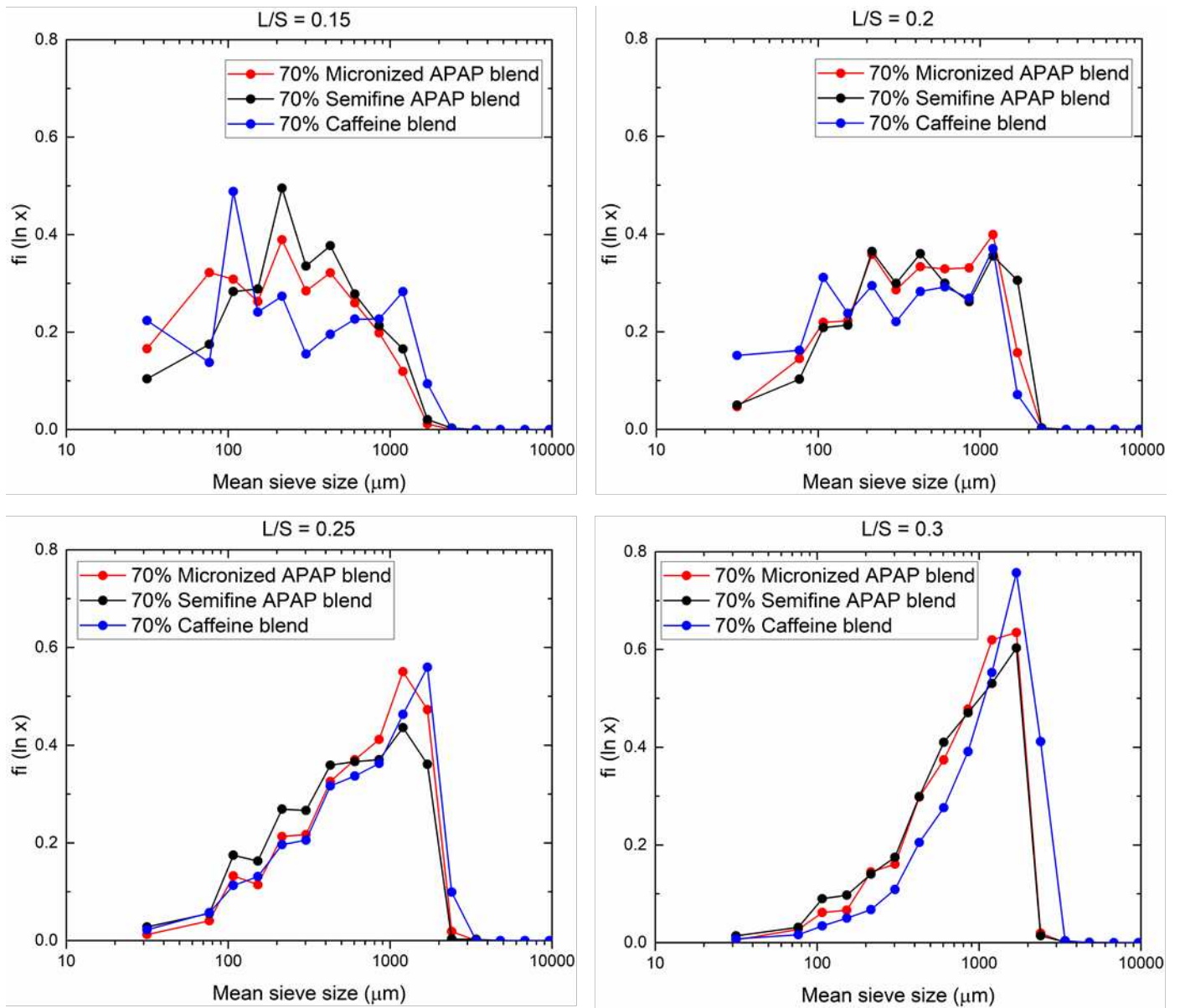


Figure 8: Granule size distributions of the 70% API blends at L/S ratios of 0.15, 0.2, 0.25, and 0.3 using distributive mixing elements.

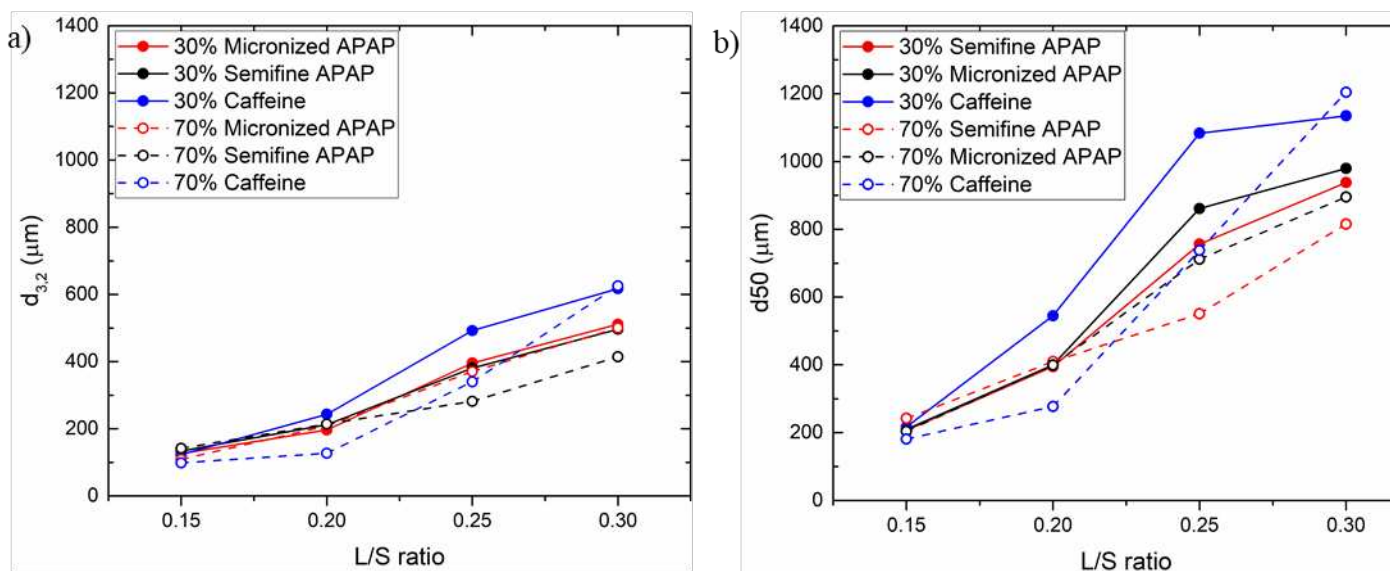


Figure 9: (a) Granule $d_{3,2}$ and (2) d_{50} values plotted as a function of L/S ratio for 30% and 70% API blends.

Source	Degrees of Freedom	Sum of Squares	F Ratio	P Value
L/S ratio	1	771231.7	411.369	0.000
API type*L/S ratio	2	23922.2	6.380	0.006
API concentration	1	10972.5	5.853	0.023
API type	2	11296.0	3.013	0.067

Table 5: Analysis of Variance results for $d_{3,2}$

Source	Degrees of Freedom	Sum of Squares	F Ratio	P Value
L/S ratio	1	2954646.5	418.138	0.000
API type	2	93636.2	6.626	0.005
API type*L/S ratio	2	86774.8	6.140	0.007
API concentration	1	53738	7.605	0.011

Table 6: Analysis of Variance results for d_{50}

It is interesting to observe the insensitivity of the granule size distribution to formulation properties for both the 30% and 70% blends despite significant differences in material DYS. The stronger caffeine blend does give slightly larger granules, but the effect is relatively small. We have shown in single granule breakage model studies that materials stronger than 9 kPa DYS do not show appreciable differences in their breakage characteristics using distributive mixing elements in TSG and their breakage probability is independent of the DYS, yielding a daughter

size distribution shape that is monomodal, representative of granule crushing [37]. In this study, the dynamic yield stress of all the blends considered have a value larger than 9 kPa for all of the L/S ratios considered. Hence, it is not surprising that granule dynamic yield strength has limited impact on the granule size distribution. It is also interesting to observe in Figures 5 and 8 that all granules are smaller than 3 mm. As explained in the literature [37], distributive mixing elements break any granules larger than 3.2 mm due to the equivalent sphere size of the maximum available free volume being equal to 3.2 mm. Thus, the granule size distributions using distributive mixing elements are a strong function of the geometry of the screw elements and depend relatively little on the formulation properties, at least for DYSs larger than a critical value (9 kPa).

An ANOVA test was performed for the d_{50} and $d_{3,2}$ of the granule size distributions at a 95% confidence interval considering API type, concentration, and L/S ratio as the source parameters (Tables 5 and 6). It was found that the L/S ratio had the largest influence on the d_{50} and $d_{3,2}$ values (p value = 0). The API type, concentration, and the interaction between API type and L/S ratio had a less significant effect on the d_{50} and $d_{3,2}$ values compared to L/S ratio. All other interaction parameters were statistically insignificant (p values $\gg 0.05$). The granule growth at increasing L/S ratios is evident in the trend of the $d_{3,2}$ and d_{50} of the granules as a function of the L/S ratio for both high and low drug dose blends (Figure 9).

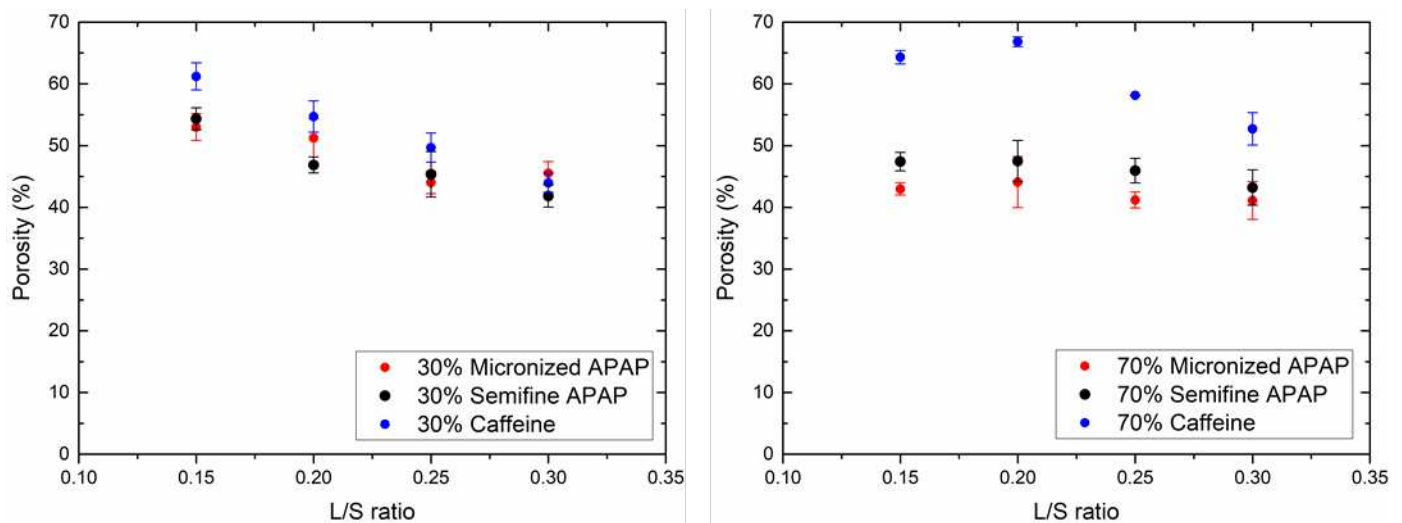


Figure 10: Granule porosity as a function of L/S ratio for 30% and 70% API blends. Points are the average of three replicate measurements with $\pm 95\%$ confidence intervals indicated by the scatter bars.

Figure 10 plots the porosities of the 30% and 70% blends as functions of the L/S ratio. All of the 30% blends show similar porosity at a given L/S ratio, whereas the 70% blends show significant differences in porosity for a given L/S ratio. The 70% caffeine blend has a larger porosity compared to the 70% APAP blends. The large difference in porosity is likely to primarily arise from the DYS of the 70% caffeine blend being significantly larger than the 70% APAP blends. Other possible contributing factors such as differences in the packing density or solubility of the API are not able to account for the large differences in porosity. Differences in the packing of the API particles within the blend can result in differences in consolidation rates, as the packing affects the minimum porosity [16,38]. However, no significant differences in bulk and tapped porosity were observed (Table 3) that can explain the large granule porosity for the 70% caffeine blend. Furthermore, normalization by the tapped bed porosity does not neutralize the differences in the granule porosity, indicating that the variation in granule porosity is not a result of differences in bed porosity. Solubility of the API in the granulating liquid can also result in decreased API availability in the solid phase during consolidation. Although caffeine shows a larger solubility in the granulating liquid than the APAP (Table 2), the difference in the amounts of API dissolved in the granulating liquid at the largest L/S ratio is only 0.3% of the total powder flow rate. This difference is not significant enough to explain such a large difference in granule porosity. It is also important to note that the 30% blends showed similar porosity values despite differences in API solubility in the granulating liquid. Thus, it is most likely that the DYS of the 70% caffeine blend, being notably larger than the 70% APAP blends, results in a larger resistance of the 70% caffeine blend to compaction. The porosity of the granules decreases as the L/S ratio increases. This observation is consistent with the literature [17]. Granules at the smallest L/S ratio have a porosity of 50% or larger, indicating that the use of distributive mixing elements does not result in dense granules.

3.3. Formulation behavior during twin screw wet granulation using distributive mixing elements

In twin screw granulation, the liquid is often added into the granulator using a drip nozzle, resulting in large nuclei sizes. The chopping and smearing of wet mass in distributive mixing elements produces excellent liquid distribution regardless of granule strength. The resulting daughter size distribution is broad and monomodal. This behavior is observed in the granule size distributions of both the low and high drug loading formulations despite a wide variation in the DYSs. While the size distribution of the granules is robust to changes in formulation properties, it is a strong function of the L/S ratio. It is important to note that granules formed using distributive mixing elements are smaller than 3.2 mm. These features result from the geometry of the screw elements as described elsewhere [37]. The granule porosity is sensitive to L/S ratio as well as the formulation's DYS. Formulations with larger DYSs have a larger resistance to granule compaction and result in more porous granules. Although consolidation models have not yet been developed specifically for twin screw granulation, the consolidation rate based on high shear granulation has been used for twin screw granulation and has an exponential dependence on the granule Stokes deformation number [38,39]. Hence, differences in material DYS will be reflected strongly in granule porosity values.

The granule size distribution and the granule porosity are strong functions of the L/S ratio during wet granulation. While the granule size distribution using distributive mixing elements is robust regardless of the type or concentration of API, the granule porosity is sensitive to the material DYS.

4. Conclusions

The effects of API particle size and concentration on the final granule attributes using distributive mixing elements are considered in this work. The key conclusions from this work are:

- 1) The type and concentration of API strongly influences the sieve analysis of dry blends due to the formation of dry API agglomerates. This effect decreases as the API concentration decreases.
- 2) The dynamic yield strengths of the caffeine blends are larger than the APAP blends and this effect is more pronounced at higher API concentrations.

- 3) Since the drop penetration times of all the formulations tested here were similar, granule differences due to differences in nucleation behavior were not observed. The effects of differences in drop penetration time in distributive mixing elements remain to be studied.
- 4) Although breakage is an important rate process in twin screw granulation, granule size distributions formed using distributive mixing elements are insensitive to variations in wet granule dynamic yield strength and are only dependent on screw element geometry and L/S ratio. The granules formed using the current distributive mixing elements are smaller than 3 mm as governed by the geometry of the screw elements.
- 5) The granule porosity is also a strong function of the L/S ratio, but unlike the granule size distribution, is dependent on the wet granule dynamic yield strength. Materials forming granules with higher dynamic yield strength form more porous granules due to having a larger resistance to granule consolidation and densification.

References:

- [1] E.I. Keleb, A. Vermeire, C. Vervaet, J.P. Remon, Twin screw granulation as a simple and efficient tool for continuous wet granulation., *Int. J. Pharm.* 273 (2004) 183–194.
doi:10.1016/j.ijpharm.2004.01.001.
- [2] N. Willecke, A. Szepes, M. Wunderlich, J.P. Remon, C. Vervaet, T. De Beer, Identifying overarching excipient properties towards an in-depth understanding of process and product performance for continuous twin-screw wet granulation, *Int. J. Pharm.* 522 (2017) 234–247. doi:10.1016/j.ijpharm.2017.02.028.
- [3] R.M. Dhenge, J.J. Cartwright, D.G. Doughty, M.J. Hounslow, A.D. Salman, Twin screw wet granulation: Effect of powder feed rate, *Adv. Powder Technol.* 22 (2011) 162–166.
doi:10.1016/j.appt.2010.09.004.
- [4] R.M. Dhenge, J.J. Cartwright, M.J. Hounslow, A.D. Salman, Twin screw wet granulation: Effects of properties of granulation liquid, *Powder Technol.* 229 (2012) 126–136.
doi:10.1016/j.powtec.2012.06.019.
- [5] R.M. Dhenge, R.S. Fyles, J.J. Cartwright, D.G. Doughty, M.J. Hounslow, A.D. Salman, Twin screw wet granulation: Granule properties, *Chem. Eng. J.* 164 (2010) 322–329.
<http://www.sciencedirect.com/science/article/pii/S1385894710004626> (accessed

November 20, 2015).

- [6] R.M. Dhenge, K. Washino, J.J. Cartwright, M.J. Hounslow, A.D. Salman, Twin screw granulation using conveying screws: Effects of viscosity of granulation liquids and flow of powders, *Powder Technol.* 238 (2013) 77–90. doi:10.1016/j.powtec.2012.05.045.
- [7] R.M. Dhenge, J.J. Cartwright, M.J. Hounslow, A.D. Salman, Twin screw granulation: steps in granule growth., *Int. J. Pharm.* 438 (2012) 20–32. doi:10.1016/j.ijpharm.2012.08.049.
- [8] D. Djuric, P. Kleinebudde, Impact of screw elements on continuous granulation with a twin-screw extruder., *J. Pharm. Sci.* 97 (2008) 4934–4942. doi:10.1002/jps.21339.
- [9] J.G. Osorio, R. Sayin, A. V. Kalbag, J.D. Litster, L. Martinez-Marcos, D.A. Lamprou, et al., Scaling of continuous twin screw wet granulation, *AIChE J.* 63 (2017) 921–932. doi:10.1002/aic.15459.
- [10] J. Vercruyssen, D. Córdoba Díaz, E. Peeters, M. Fonteyne, U. Delaet, I. Van Assche, et al., Continuous twin screw granulation: Influence of process variables on granule and tablet quality, *Eur. J. Pharm. Biopharm.* 82 (2012) 205–211. doi:10.1016/j.ejpb.2012.05.010.
- [11] M.R. Thompson, J. Sun, Wet granulation in a twin-screw extruder: implications of screw design, *J. Pharm. Sci.* 99 (2010) 2090–2103. doi:10.1002/jps.21973.
- [12] M.R. Thompson, Twin screw granulation – review of current progress, *Drug Dev. Ind. Pharm.* 0 (2014) 1–9. doi:10.3109/03639045.2014.983931.
- [13] R. Sayin, A.S. El Hagrasy, J.D. Litster, Distributive mixing elements: Towards improved granule attributes from a twin screw granulation process, *Chem. Eng. Sci.* 125 (2015) 165–175. doi:10.1016/j.ces.2014.06.040.
- [14] A.S. El Hagrasy, J.D. Litster, Granulation rate processes in the kneading elements of a twin screw granulator, *AIChE J.* 59 (2013) 4100–4115. doi:10.1002/aic.14180.
- [15] H. Li, M.R. Thompson, K.P. O’Donnell, Understanding wet granulation in the kneading block of twin screw extruders, *Chem. Eng. Sci.* 113 (2014) 11–21. doi:10.1016/j.ces.2014.03.007.

- [16] J. Litster, B.J. Ennis, Ennis, Litster - The Science and Engineering of Granulation Processes, 2004.
- [17] A.S. El Hagrasy, J.R. Hennenkamp, M.D. Burke, J.J. Cartwright, J.D. Litster, Twin screw wet granulation: Influence of formulation parameters on granule properties and growth behavior, *Powder Technol.* 238 (2013) 108–115. doi:10.1016/j.powtec.2012.04.035.
- [18] H.N. Emady, D. Kayrak-Talay, J.D. Litster, Modeling the granule formation mechanism from single drop impact on a powder bed, *J. Colloid Interface Sci.* 393 (2013) 369–376. doi:10.1016/j.jcis.2012.10.038.
- [19] S.M. Iveson, J.A. Beathe, N.W. Page, The dynamic strength of partially saturated powder compacts: the effect of liquid properties, *Powder Technol.* 127 (2002) 149–161. doi:10.1016/S0032-5910(02)00118-3.
- [20] S.M. Iveson, N.W. Page, Brittle to Plastic Transition in the Dynamic Mechanical Behavior of Partially Saturated Granular Materials, *J. Appl. Mech.* 71 (2004) 470. doi:10.1115/1.1753269.
- [21] S.M. Iveson, N.W. Page, J.D. Litster, The importance of wet-powder dynamic mechanical properties in understanding granulation, *Powder Technol.* 130 (2003) 97–101. doi:10.1016/S0032-5910(02)00233-4.
- [22] R.M. Smith, L.X. Liu, J.D. Litster, Breakage of drop nucleated granules in a breakage only high shear mixer, *Chem. Eng. Sci.* 65 (2010) 5651–5657. doi:10.1016/j.ces.2010.06.037.
- [23] E.I. Keleb, a Vermeire, C. Vervaet, J.P. Remon, Extrusion granulation and high shear granulation of different grades of lactose and highly dosed drugs: a comparative study., *Drug Dev. Ind. Pharm.* 30 (2004) 679–691. doi:10.1081/DDC-120039338.
- [24] S. Yu, G.K. Reynolds, Z. Huang, M. de Matas, A.D. Salman, Granulation of increasingly hydrophobic formulations using a twin screw granulator., *Int. J. Pharm.* 475 (2014) 82–96. doi:10.1016/j.ijpharm.2014.08.015.
- [25] H. Li, M.R. Thompson, K.P. O'Donnell, Examining Drug Hydrophobicity in Continuous Wet Granulation within a Twin Screw Extruder, *Int. J. Pharm.* 496 (2015) 3–11.

- doi:10.1016/j.ijpharm.2015.07.070.
- [26] M.R. Thompson, S. Weatherley, R.N. Pukadyil, P.J. Sheskey, Foam granulation: new developments in pharmaceutical solid oral dosage forms using twin screw extrusion machinery, *Drug Dev. Ind. Pharm.* 38 (2012) 771–784.
<http://www.tandfonline.com/doi/full/10.3109/03639045.2011.633265#.Vk99nfmrTIU>
(accessed November 20, 2015).
- [27] M.R. Thompson, B. Mu, P.J. Sheskey, Aspects of foam stability influencing foam granulation in a twin screw extruder, *Powder Technol.* 228 (2012) 339–348.
doi:10.1016/j.powtec.2012.05.050.
- [28] K.E. Rocca, S. Weatherley, P.J. Sheskey, M.R. Thompson, Influence of filler selection on twin screw foam granulation., *Drug Dev. Ind. Pharm.* 9045 (2013) 35–42.
doi:10.3109/03639045.2013.845839.
- [29] M. Fonteyne, A. Correia, S. De Plecker, J. Vercruyssen, I. Ilić, Q. Zhou, et al., Impact of microcrystalline cellulose material attributes: A case study on continuous twin screw granulation, *Int. J. Pharm.* 478 (2015) 705–717. doi:10.1016/j.ijpharm.2014.11.070.
- [30] S.H. Yalkowsky, Y. He, *Handbook of Aqueous Solubility Data*, CRC Press, 2003.
<http://www.crcnetbase.com.ezproxy.lib.purdue.edu/doi/pdfplus/10.1201/9780203490396.ch1>
(accessed April 12, 2017).
- [31] R.A. Granberg, A.C. Rasmuson, Solubility of Paracetamol in Pure Solvents, *J. Chem. Eng. Data.* 44 (1999) 1391–1395. doi:10.1021/JE990124V.
- [32] L.X. Liu, R. Smith, J.D. Litster, Wet granule breakage in a breakage only high-shear mixer: Effect of formulation properties on breakage behaviour, *Powder Technol.* 189 (2009) 158–164. doi:10.1016/j.powtec.2008.04.029.
- [33] A.L.H. Tran, *Powder Flow In Vertical High Shear Mixer Granulators*, The University of Queensland, 2015.
https://espace.library.uq.edu.au/data/UQ_349856/s354369_phd_submission.pdf?Expires=1493926157&Signature=hm3dPTBtGYNC63HibJmLiRnrgIGIZOBkP2Hb5RYr-N2pCTLbNDL7CorMRmaTs1HL2~yEhyMmSAdiKz1Y5dwjxFDXxbR18GzvD6hOMib

- yUKpbsWBiaGudlV86Gdv1Iu-jxpdKWZDiyhZsLnzzlQwjy2R (accessed May 3, 2017).
- [34] R.M. Smith, *Wet Granule Breakage in High Shear Mixer Granulators*, (2007).
<http://espace.library.uq.edu.au/view/UQ:151724> (accessed November 20, 2015).
- [35] S.U. Pradhan, Y. Zhang, J. Li, J.D. Litster, C.R. Wassgren, Tailored Granule Properties Using 3D Printed Screw Geometries in TSG, *Submitt. to Powder Technol.* (n.d.).
- [36] M. De Matas, H.G.M. Edwards, E.E. Lawson, L. Shields, P. York, FT-Raman spectroscopic investigation of a pseudopolymorphic transition in caffeine hydrate, *J. Mol. Struct.* 440 (1998) 97–104. doi:10.1016/S0022-2860(97)00231-7.
- [37] S.U. Pradhan, M. Sen, J. Li, J.D. Litster, C.R. Wassgren, Granule breakage in twin screw granulation: Effect of material properties and screw element geometry, *Powder Technol.* 315 (2017) 290–299. doi:10.1016/j.powtec.2017.04.011.
- [38] S.M. Iveson, J.D. Litster, Fundamental studies of granule consolidation part 2: Quantifying the effects of particle and binder properties, *Powder Technol.* 99 (1998) 243–250. doi:10.1016/S0032-5910(98)00116-8.
- [39] D. Barrasso, T. Eppinger, F.E. Pereira, R. Aglave, K. Debus, S.K. Bermingham, et al., A multi-scale, mechanistic model of a wet granulation process using a novel bi-directional PBM–DEM coupling algorithm, *Chem. Eng. Sci.* 123 (2015) 500–513.
doi:10.1016/j.ces.2014.11.011.